Effect of Nanosize $CaSO_4$ and $Ca_3(PO_4)_2$ Particles on the Rheological Behavior of Polypropylene and Its Simulation with a Mathematical Model

S. Mishra,[1] Shirish Sonawane,[1] Arindam Mukherji,[1] H. C. Mruthyunjaya[2]

[1]*Department of Chemical Technology, North Maharashtra University, Jalgaon, P.O. Box 80, Maharashtra State, India 425001*
[2]*Jain Irrigation Systems, Ltd., Jalgaon, Maharashtra State, India 425001*

Received 27 December 2004; accepted 8 July 2005
DOI 10.1002/app.23595
Published online in Wiley InterScience (www.interscience.wiley.com).

ABSTRACT: Nanosize $CaSO_4$ and $Ca_3(PO_4)_2$ fillers were synthesized with an in situ deposition technique, and their sizes were confirmed by X-ray diffraction. $CaSO_4$ was prepared in 12- and 22-nm sizes, and $Ca_3(PO_4)_2$ was prepared in 13- and 24-nm sizes. Experimental variables, such as torque, shear viscosity, shear stress, and shear rate, of the nanofilled polypropylene (PP) composites were measured with torque rheometry and melt flow index (MFI) measurements. Torque versus time, shear viscosity versus weight percentage, and MFI versus weight percentage were plotted to investigate the rheological behavior of the nanofilled composites. The Cross–Williamson (CW) model was simulated with the MATLAB simulation package to study the thinning behavior of the PP composites. The experimental results show a decrease in the shear viscosity with increasing weight percentage of filler. Shear thinning in the molten PP composites was comparatively greater with decreasing nanosize of $CaSO_4$ and $Ca_3(PO_4)_2$. This kind of behavior was confirmed by the N parameter as determined from the CW model. The simulation of experimental data also showed similar trends as the theoretical data. At a certain stage, a violation of theoretical data was observed. This was because of practical limitations of the equation, as the equation does not include consideration of the physical situation of chain entanglements. © 2006 Wiley Periodicals, Inc. J Appl Polym Sci 100: 4190–4196, 2006

Key words: nanoparticles; polypropylene (PP); rheology; shear

INTRODUCTION

Polymer composites filled with nanoparticles have been extensively studied recently; they often exhibit drastic changes in the rheological and mechanical properties in comparison to microparticle composites.[1–6] The improvement of properties of nanocomposites basically depends on structure, surface area of nanoparticles and interfacial bonding, in case of clay nanoparticles with polymer matrix. The combination of clays and functional polymers interacting at atomic level constitutes the basis for preparing an important class of inorganic–organic nonstructural materials. Platelets of nanoclay particles such as montmorillonite clay and vermiculite have highest aspect ratio (more than 300). Low-energy materials such as polyethylene (PE) and polypropylene (PP) interact weakly with mineral surfaces; thus, the synthesis of polyolefin nanocomposites by melt compounding is considerably more difficult. Gopakumar et al.[7] observed that PE/clay composites behaved in a similar manner to conventional composites with a modest increase in their rheological properties and Young's modulus. Conversely, the nanoscale dimensions of the dispersed clay platelets in the nanocomposites led to a significant increase in the viscous and elastic properties and an improved stiffness. There are two possibilities for creating microstructures: one is intercalation, and the other is exfoliation. Intercalated nanocomposites are generally obtained when the polymer is located between the silicate layers. Although the layer spacing is increasing, attractive forces between the silicate layers and stack layers are uniform. Exfoliated structures are formed when the layer spacing increases to the point where there are no longer sufficient attractions between those silicate layers to maintain uniform layer spacing. Intercalated and exfoliated polystyrene (PS)/clay nanocomposites have been widely investigated for the melt intercalation of PS into organically modified sodium bentonite.[8] Hoffmann et al.[9] reported a correlation between the morphology and rheology of

Part of this article was presented at the MACRO-2004 International Conference on Polymers for Advanced Technologies, December 2004, Thiruvananthapuram, India.
Correspondence to: S. Mishra (profsm@rediffmail.com).
Contract grant sponsor: Department of Science and Technology, New Delhi; contract grant number: SR/S-5 WM-31/2003.

exfoliated PS nanocomposites based on organophillic silicate layers such as flouromicas. Okamoto et al.[10] studied the rheological properties of biodegradable polycaprolactone and poly(butylene succinate); they observed that the rheological behaviors of the nanocomposites were significantly affected by the degree of dispersion of the organoclay.

A poly(methyl methacrylate)/nano-$CaCO_3$ nanocomposite system was studied by Qiang et al.[11] with the reverse microemulsion method. They found that the aqueous layer and modification of surface of nano-$CaCO_3$ with polyacrylamide did not significantly change the surface area of the nanoparticles. Nanocomposites of poly(vinyl chloride) and nano-$CaCO_3$ with chlorinated polyethylene (PE) was studied by Wang et al.[12]

In this study, we dealt with the structural effect of two different nanosizes of $CaSO_4$ and $Ca_3(PO_4)_2$ on rheological behavior. Hence, rheological parameters such as torque, shear rate, and shear viscosity were determined with a rheometer and a melt flow apparatus.

EXPERIMENTAL

Materials

PP [grade 310367 (REPOL); melt flow index (MFI) = 8.94 g/10 min; density = 0.92 g/cc] was procured from Reliance Industries, Ltd. (Mumbai, India). Analytical grades of calcium chloride, ammonium sulfate, diammonium hydrogen phosphate, and poly(ethylene glycol) (PEG; molecular weight = 6000), procured from Qualigens India, Ltd. (Mumbai, India), were used for the synthesis of nanoparticles of calcium sulfate and calcium phosphate.

Nanoparticle synthesis

The nanosize calcium sulfate was synthesized by an in situ deposition technique. Calcium chloride (110 g) was added to 140 mL of water. PEG (248 g) was diluted in 200 mL of water and mildly heated for proper mixing. The complex of calcium chloride and PEG was prepared in 1:4 and 1:20 molar ratios. We prepared another solution of ammonium sulfate by adding 132 g to 80 mL of water. The first complex of PEG and calcium chloride solution was digested for 12 h; then, a second solution was added slowly and kept for digestion overnight. The precipitate was filtered, washed with water, and dried in vacuo. With the same molar ratios and preparation method, ammonium phosphate was used in place of ammonium sulfate for the synthesis of nano calcium phosphate.[11–18] The viscosity of the PEG solution was measured by Bubble Gardner tubes to confirm the possible thickening of the water-soluble matrix. The yields of calcium phosphate and calcium sulfate, respectively, were recorded as 65 and 87% in the 4:1 molar ratio and 55 and 65% in 20:1 molar ratios. The method of nanosynthesis is given in Figure 1.

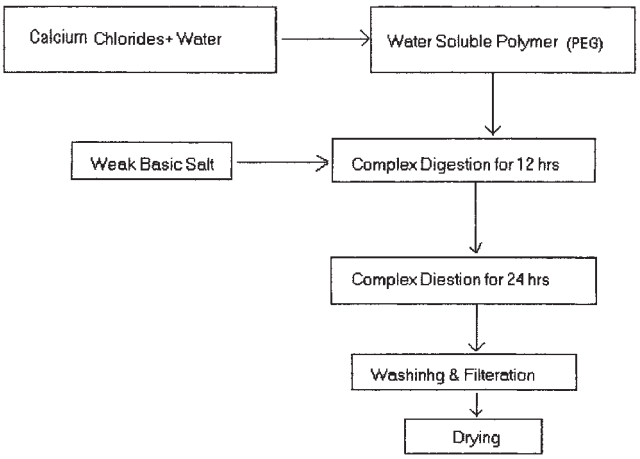

Figure 1 In situ deposition technique for the nanosynthesis of $CaSO_4$ and $Ca_3(PO_4)_2$.

Sample preparation for characterization

PP granules and nanoparticles in different weight percentages were premixed in a Rheomix 600 mixer (Haake Rheocord 900, Dieselstrasse, Germany). The temperatures of the feed zone, compression zone, metering zone, and die were 215, 215, 215, and 220°C, respectively. The die gap, the diameter of the screw, and length of the screw were 1, 19.1, and 477.5 mm, respectively. The 50-rpm speed was kept constant for 10 min. The torque value was measured at a span of 15 s for each sample. The data was converted into torque values with following equation.

$$\tau = I/K$$

$$I = \text{Current } (mA)$$

$$K = \text{torque constant} = 1.223$$

where τ is the torque, I is the current (mA), and K is the torque constant ($K = 1.223$).

MFI measurements

The sample material mixed with nanoparticles obtained from the Rheomix 600 mixer was used for MFI measurement. MFI measurements were done per ASTM D 1238 on the melt flow meter (Ceast, S.PA. Torin, Italy). The load applied was 21.18 N at a tem-

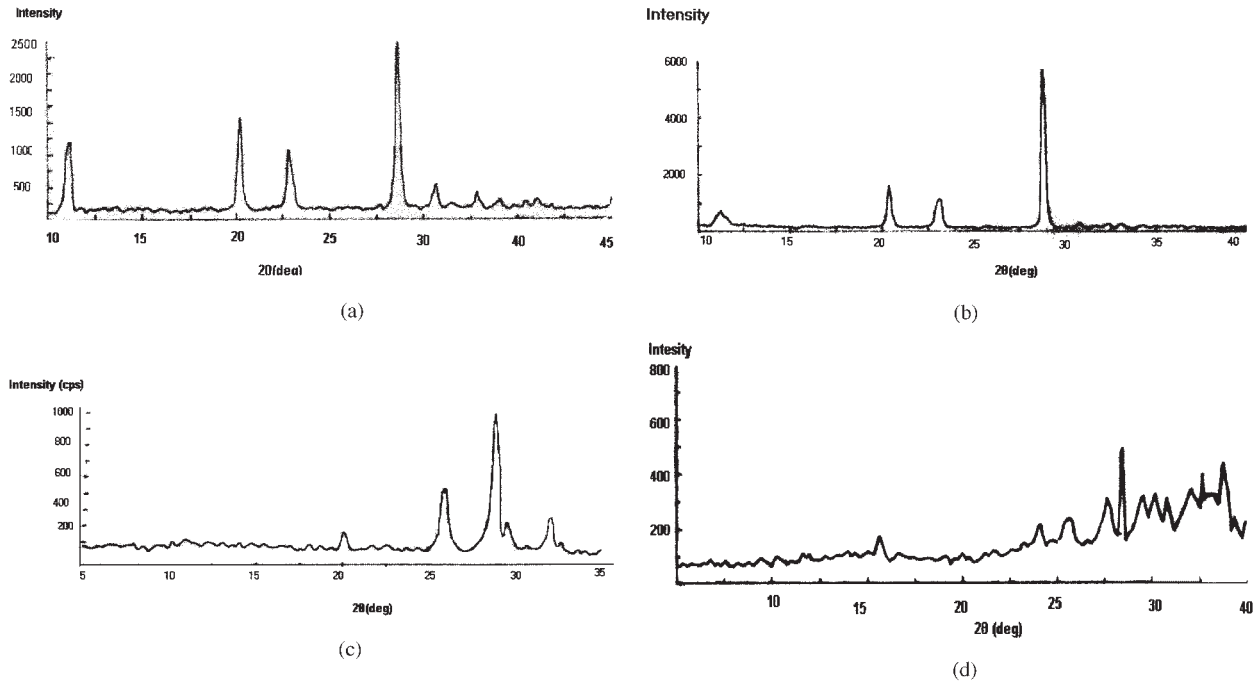

Figure 2 X-ray diffractograms of (a) 12- and (b) 22-nm $CaSO_4$ and (c) 13- and (d) 24-nm $Ca_3(PO_4)_2$.

perature of 230°C, with a measuring length of 25.40 mm and a nozzle diameter of 2.095 mm. Rheological data (g/10 min) was generated for 10 units of each sample. The melt flow average and standard deviation were also measured for each sample.

X-ray diffraction (XRD)

The nanosizes were confirmed by an X-ray diffractometer (Rigaku model, Tokyo, Japan) with the intensity maintained in the range 0–6000 Cps and at a diffraction angle of 0–35°.

Differential scanning calorimetry (DSC)

The crystallization behavior of the PP composites was recorded on a PerkinElmer (Wellesley, MA) differential scanning calorimeter. Crystallization was studied in the range 50–400°C at a rate of 10°c/min in a nitrogen environment. Furthermore, to ensure complete melting, the sample was held for 1 min at 400°C and then cooled to 50°C at the same rate.

Mathematical modeling and parameter calculation

The Cross–Williamson (CW) model[8] was used to establish a relationship between shear rate and shear viscosity of the resin matrix (dispersion phase) and the resin filled with $CaCO_3$ (dispersed phase). It is given as follows:

$$\eta = \eta_0/(1 + |\lambda\gamma|^{1-N}) \quad (1)$$

where η_0 is the zero shear viscosity [$\eta_0 = \text{Lim}\ \eta(\gamma)$], λ is the characteristic time of the nanocomposites (s), γ is the shear viscosity (Pa s), and N is a dimensionless parameter.

RESULTS AND DISCUSSION

XRD characterization of the nano-$CaSO_4$ and nano-$Ca_3(PO_4)_2$ particles

Figure 2(a–d) shows XRD scans of the $CaSO_4$ synthesized in PEG. Figure 2(a,b) shows that with increasing concentration of PEG, the nanosize of $CaSO_4$ decreased. The particle sizes of different ratios of PEG and calcium chloride (1:4 and 1:20) were recorded as 22 and 12 nm for $CaSO_4$ and 24 and 13 nm for $Ca_3(PO_4)_2$, respectively. Figure 2(c,d) shows the X-ray diffractograms of $Ca_3(PO_4)_2$. The size of the nanoparticles (d) was confirmed with Scherer's formula, which is given as follows:

$$d(\text{Å}^\circ) = k\lambda/\Delta 2\theta\cos\theta$$

K = Order of Reflection

$\lambda = 1.542$

θ = Diffraction Angle

$$\Delta 2\theta = \text{Full width at Half Maximum (FWHM)}$$

where K is the order of reflection, $\lambda = 1.542$, θ is the diffraction angle, and $\Delta 2\theta$ is the full width at half-maximum.

With increasing concentration of the water-soluble polymer, the XRD peaks became broader, which was a major indication of a reduction in nanosize. The broadening of the peak may have been due to vigorous mixing at the molecular level. It has been reported[18] that the usual precipitation method is not suitable for constraining the phases; even small changes in the temperature also cause variation in nanosize and structure for both cases, that is, in situ deposition and conventional precipitation methods. So we used the in situ deposition method at the normal temperature by cooling a hot-water-soluble mixture to room temperature.

Effect of the nanoparticles on the thermal properties of the PP nanocomposites

Figure 3(a,b) shows the DSC thermograms of virgin PP and composites containing nano-$CaSO_4$ and nano-$Ca_3(PO_4)_2$ with various weight percentages and a reduction in nanosize. The heat of fusion (ΔH) decreased with increasing weight percentage of $CaSO_4$. A similar effect of the absorption of heat was also observed for the $Ca_3(PO_4)_2$ composites. In both kinds of composite, the absorption of heat energy increased with a reduction in the nanosize of the fillers. This was due to a higher increment in the surface area of the nanoparticles. The structural effect of both kinds of nanoparticle also showed a difference in the heat of absorption. $CaSO_4$ has a needlelike structure, and $Ca_3(PO_4)_2$ has a spherical structure.[13,17] The $Ca_3(PO_4)_2$ composites showed an almost higher absorption of heat energy compared to the $CaSO_4$ composites. This was evidence of the structural morphology of the particles when they were added to the composites. The melting point showed a marginal increase in value, for example, for virgin PP melts at 162.16°C, and all composites showed melting points in the range 162–163°C. As the addition of nanoparticles was very small (0.1–0.5 wt %) in amount, it was obvious that the melting temperatures were not much affected.

Variation of the torque with time for different nanosizes of the PP/nano-$CaSO_4$ and PP/nano-$Ca_3(PO_4)_2$ composites

The difference in the decrement in the torque requirement with time for virgin PP and its nano-$CaSO_4$ composite was more pronounced for the 12-nm $CaSO_4$ compared to the 22-nm $CaSO_4$ (Fig. 4). However, as the particle size increased, the initial requirement of torque to incorporate the filler into the matrix was more than that of the smaller nanosize particles. When

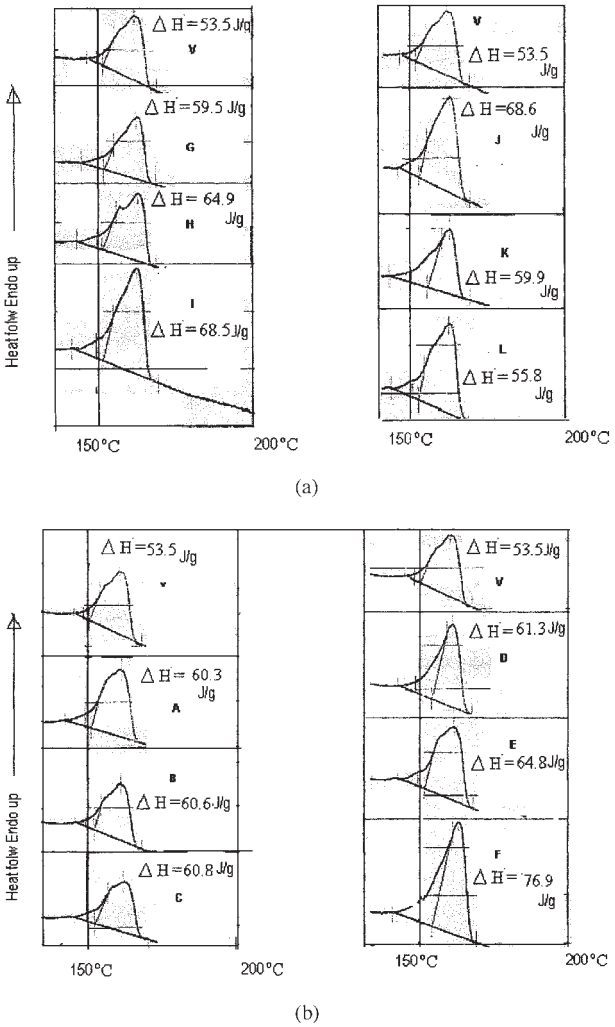

Figure 3 DSC thermograms of (a) nano-$CaSO_4$/PP composites of (V) virgin PP; (G) 0.5, (H) 0.3, and (I) 0.1 wt % 12-nm $CaSO_4$; and (J) 0.5, (K) 0.3, and (L) 0.1 wt % 220-nm $CaSO_4$ and (b) nano-$Ca_3(PO_4)_2$/PP composites of (V) virgin PP; (A) 0.5, (B) 0.3, and (C) 0.1 wt % 13-nm $Ca_3(PO_4)_2$; and (D) 0.5, (E) 0.3, and (F) 0.1 wt % 24-nm $Ca_3(PO_4)_2$.

we compared the two nanosizes of $CaSO_4$, we noted that the torque, recorded during the mixing of the reduced nanosize particles, lasted for a longer time compared to that of the bigger nanosize and virgin PP. This might have been due to the dispersion of smaller nanoparticles that closely bound the matrix and, hence, created a restriction to flow with less variation in torque during processing. The same was also observed for $Ca_3(PO_4)_2$ in PP for various nanosizes (Fig. 5).

Effect on viscosity of the weight percentages of nano-$CaSO_4$ and nano-$Ca_3(PO_4)_2$ in the composites

Figure 6(a) and Table I show that the shear viscosity decreased with increasing weight percentage of 24- and 13-nm $Ca_3(PO_4)_2$. The shear viscosities observed,

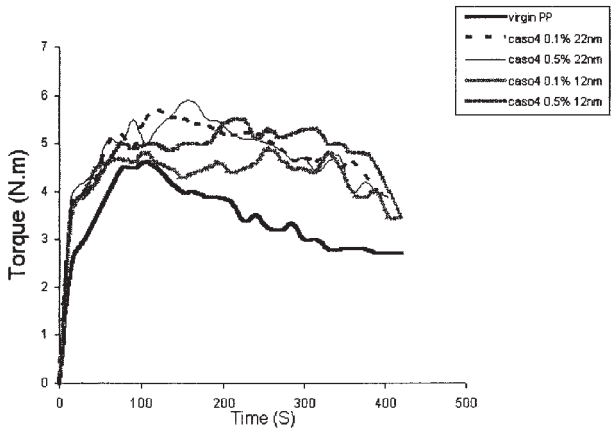

Figure 4 Torque required to process 22- and 12-nm $CaSO_4$ at different filler compositions in PP.

1010 and 826 Pa S for 13- and 24-nm $Ca_3(PO_4)_2$, respectively, were less than that of virgin PP (1100 Pa S) [Fig. 6(a)]. Thus, the addition in lesser amounts (0.1–0.5 wt %) of nano-$Ca_3(PO_4)_2$ caused drastic changes in the rheological properties. Wang et al.[12] also added chlorinated PE to improve the rheological properties of poly(vinyl chloride)/nano-$CaCO_3$. For nano-$CaSO_4$, an increase in shear viscosity was observed up to 0.4 wt % of its addition. The shear viscosities were recorded as 862.5 and 1138.5 Pa S, respectively, for a 0.5 wt % loading of 22-nm $CaSO_4$ and a 0.4 wt % loading of 12-nm $CaSO_4$ in the composites [Fig. 6(b)].

As shown by the values of the *N* parameter in Table I and Figure 6(a,b), shear thinning was observed for the $Ca_3(PO_4)_2$ nanoparticles, where smaller particle sizes showed less shear thinning in comparison to bigger nanoparticles for the same weight percentage. Like nano-$Ca_3(PO_4)_2$, the smaller nanosize (12 nm) of $CaSO_4$ showed shear thinning on its addition at 0.1 wt % in the composites, and a shear thickening phenomena was observed at higher weight percentages, which was, however, less than 1. Shear thinning was observed from 0.1 to 0.5 wt % for 22-nm $CaSO_4$. This behavior was due to the needlelike structure of $CaSO_4$, so the adherence of the polymer chains on continuously dispersed smaller nanoparticles of $CaSO_4$ formed a needlelike structure, which was responsible for creating a hindrance of movement in the chains at a higher rate. Although for the bigger sizes of $CaSO_4$, the needle shape became somewhat oval; hence, the movement of the chains became easy. Such a phenomena was also observed for $Ca_3(PO_4)_2$, where the particle shape was spherical, and therefore, $Ca_3(PO_4)_2$ shows higher shear thinning compared to $CaSO_4$.

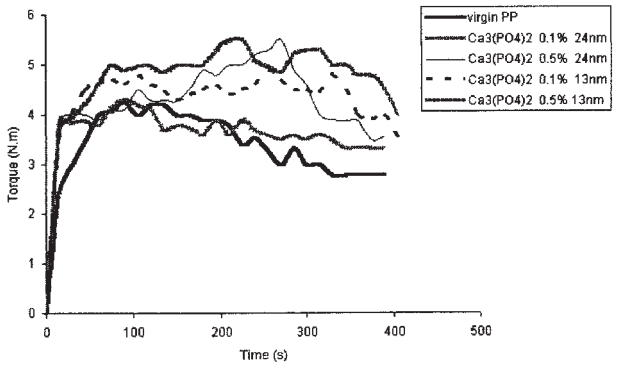

Figure 5 Torque required to process different 24- and 12-nm $Ca_3(PO_4)_2$ filler compositions in PP.

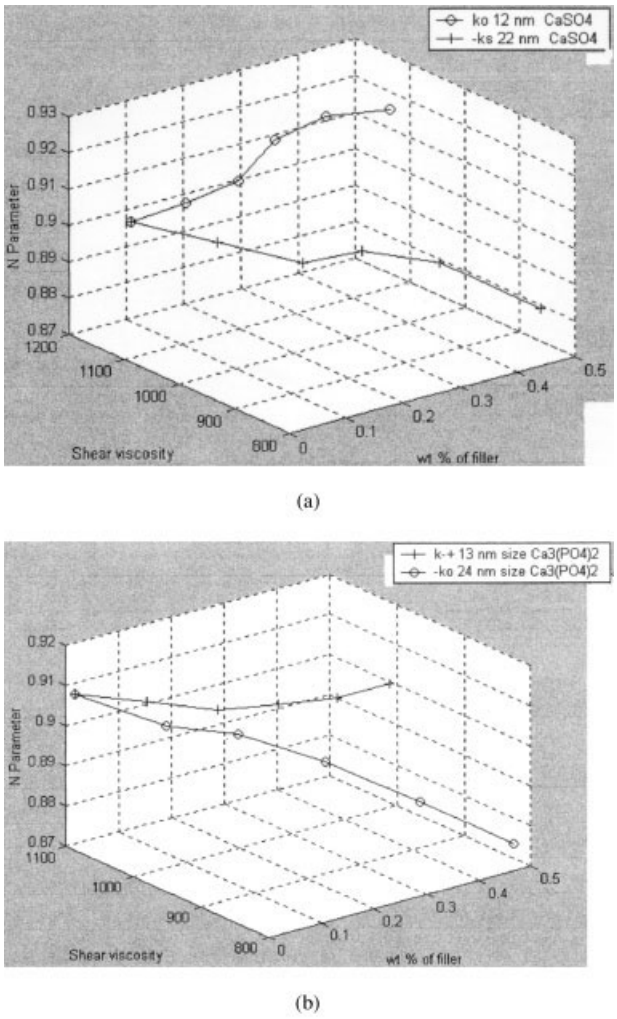

Figure 6 Variation of *N* values and weight percentage against shear viscosity in (a) 12- and 22-nm $CaSO_4$ and (b) 13- and 24-nm $Ca_3(PO_4)_2$.

Effect on MFI of the weight percentages of nano-$CaSO_4$ and nano-$Ca_3(PO_4)_2$ in the composites

As shown in Figure 7, the 22-nm $CaSO_4$ showed higher values of MFI than the 12-nm size for the same amount in the composites. The maximum MFI was

TABLE I
***N* Parameter, Shear Rate, and Shear Viscosity Values for Various Filler Contents**

Filler (wt%)	*N* parameter	Shear rate	γ	γ theoretical value
13-nm $Ca_3(PO_4)_2$				
0.0	0.909	17.939	1085.935	1088.7
0.1	0.9056	18.4	1058.756	1068.9
0.2	0.9021	18.9	1030.634	1045.2
0.3	0.9007	19.021	1020.441	1039.5
0.4	0.8995	19.228	1011.021	1032.2
0.5	0.8995	19.39	1010.4	1031.6
24-nm $Ca_3(PO_4)_2$				
0.0	0.909	17.939	1085.935	1088.7
0.1	0.9018	18.939	1028.591	1045.7
0.2	0.8982	19.45	1000.611	1024.3
0.3	0.8918	21.241	950.124	983.88
0.4	0.8828	21.928	888.401	933.11
0.5	0.8737	23.726	826.01	879.49
12-nm $CaSO_4$				
0.0	0.909	17.939	1085.935	1088.7
0.1	0.9095	17.81	1090.14	1092.1
0.2	0.9107	17.64	1100.001	1104
0.3	0.9152	17.119	1137.971	1126.2
0.4	0.9165	16.96	1148.897	1134.1
0.5	0.9151	17.44	1135.4775	1124.6
22-nm $CaSO_4$				
0.0	0.909	17.939	1085.935	1088.7
0.1	0.903	18.828	1034.638	1050.2
0.2	0.896	19.802	983.749	1010.9
0.3	0.896	19.680	979.001	1007.1
0.4	0.891	20.670	942.462	977.9
0.5	0.879	22.588	862.423	911.19

recorded at 0.5 wt % of the 22-nm $CaSO_4$. The 12-nm $CaSO_4$ did not show an increase in MFI with increasing weight percentage of filler; on the contrary, the MFI value decreased up to 0.4 wt % and then stabilized. The MFI values for 12- and 22-nm of $CaSO_4$ were recorded as 8.90 and 11.26 g/10 min, respectively, which were greater than the value for virgin PP (8.6 g/10 min). The increase in MFI in both nanoparticle sizes of $Ca_3(PO_4)_2$ was not sharp up to 0.3 wt % filler. The MFI for the 13-nm $Ca_3(PO_4)_2$ was lower than for the 24-nm size. The overall increase for the 13-nm $Ca_3(PO_4)_2$ was 9.8, whereas it was 11.8 for the 24-nm $Ca_3(PO_4)_2$. This was due to the structure of the nanoparticles, which played an important role in the rheology and was discussed in earlier part of this article.

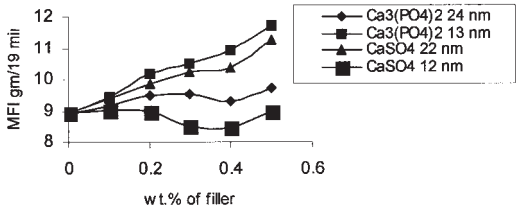

Figure 7 Variation in MFI of two different nanosizes of $CaSO_4$ and $Ca_3(PO_4)_2$ at different weight percentages.

Mathematical modeling of the rheology of nano-$CaSO_4$ and nano-$Ca_3(PO_4)_2$ in the PP matrix

The CW model was applied to examine the relationship between the shear viscosity and shear rate.[8] This model accounts for the shear rate dependence of viscosity. The experimental data were fitted to the model, and *N* dimensionless parameters were calculated. *N* values above 1 indicated shear thickening, and *N* values below 1 indicated shear thinning of the pure and nanofilled PP composites. Figure 6 and Table I show *N* against shear viscosity, which confirmed the shear thinning and thickening behaviors of nanofilled PP composites. There was shear thinning for both nanofillers, but 12 nm of $CaSO_4$ showed comparative shear thickening (as discussed earlier). The experimental and theoretical data of shear viscosity, shear rate, and variation in amount of $CaSO_4$ and $Ca_3(PO_4)2$ are shown in Table I and Figure 8(a,b), which are similar in trend, but the CW equation identified the situations at the lower and higher shear rates obtained experimentally and theoretically. This difference was due to the limitations of the CW model equation, as the model equation could not account for such a kind of practical situation.

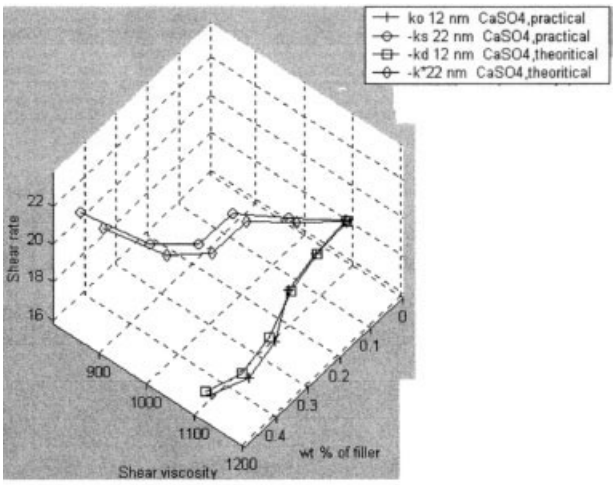

(a)

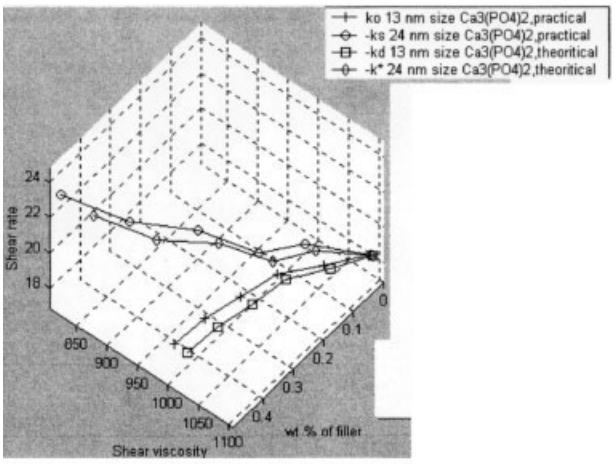

(b)

Figure 8 Experimental versus theoretical data of (a) 12- and 22-nm filled $CaSO_4$ and (b) 13- and 24-nm $Ca_3(PO_4)_2$ at different shear rates.

CONCLUSIONS

The thermal behavior of the nanofilled composites also favored the absorption of heat energy with increasing weight percentage and decreasing nanosize of filler. The reduction in nanosize favored shear thickening in both $CaSO_4$ and $Ca_3(PO_4)_2$. The shear viscosity versus weight percentage of filler and the MFI versus weight percentage of filler were almost opposite each other, which also confirmed the results of shear thinning with increasing weight percentage of filler. The experimental results obey the CW model.

References

1. Kalgaonkar, J. J. P. J Polym Sci Part B: Polym Phys 2001, 39, 446.
2. Whiteside, G. M.; Mathias, T. P.; Seto, C. T. Science 1991, 254, 1312.
3. Novak, B. Adv Mater (Weinheim, Germany) 1993, 5, 422.
4. Vaia, R. A.; Giannelis, E. P. Macromolecules 1997, 30, 8000.
5. Vaiva, R. A.; Ishii, H.; Giannelis, E. P. Chem Mater 1995, 5, 1694.
6. Mishra, S.; Sonawane, S. H.; Singh, R. P.; Bendale, A.; Patil, K. J Appl Polym Sci 2004, 94, 116.
7. Gopakumar, T. G.; Lee, J. A.; Kontopoulou, M.; Parent, J. S. Polymer 2002, 43, 5483.
8. Kim, T. H.; Jang, L. W.; Lee, D. C.; Choi, H. J.; Jhon, M. S. Macromol Rapid Commun 2002, 23, 191.
9. Hoffmann, B.; Dietrich, C.; Thomann, R.; Friedrich, C.; Mullhaupt, R. Macromol Rapid Commun 2000, 21, 57.
10. Okamoto, K.; Ray, S. S.; Okamoto, M. J Polym Sci Part B: Polym Phys 2003, 41, 3160.
11. Qiang, X.; Zhao, C.; Yuan, J.; Cheng, S. Y. J Appl Polym Sci 2004, 91, 2739.
12. Wang, X.; Wu, D.; Song, Y.; Jin, R. J Appl Polym Sci 2004, 92, 2717.
13. Radhakrishnan, S.; Saujanya, C. J Mater Sci 1998, 33, 1069.
14. Godvski, Yu, D. Adv Polym Sci 1999, 119, 79.
15. Sherman, L. M. Plast Technol 1999, 45(6), 53.
16. Atozi, M.; Rundle, J. Chem Phys 1958, 29, 1306.
17. Saujanya, C.; Radhakrishanan, S. Polymer 2001, 42, 6723.
18. Herist, C.; Mathieu, J. P.; Vogels, C.; Rulmont, A.; Cloots, R. J Cryst Growth 2003, 249, 321.